TriboBR
First International Brazilian Conference on Tribology – TriboBr-2010 and ITS - IFToMM 2010 - 2nd International Tribology Symposium of IFToMM
24th to 26th november, 2010
Copacabana, Rio de Janeiro/RJ, Brazil
ISSN 2179-3956

THE INFLUENCE OF CONTACT STRESS DISTRIBUTION ON TOOTH FLANK OF SPUR GEAR AND SPECIFIC FILM THICKNESS IN WEAR RESISTANCE DURING PITTING TESTS[1]

Marco Antonio Muraro [2]
Urbano Reisdorfer Junior [3]
Fábio Koda [4]
Carlos Henrique da Silva [5]

Abstract
One of the main gear damage mechanisms is the formation of pitting and spalling on the tooth flank. Several factors have significant influence on the formation of such damage, such as: level of tension at the contact; tooth profile type; relative contact velocities; surface finish and lubrication conditions. This work comprehends the global observation of all such parameters, carried out to explain the phenomena related to this wear mechanism. The test equipment uses the power recirculation principle, and is commonly known as FZG test rig. The gear has C-type geometry with modified profile. The gears were made from AISI 8620 steel and had two types of surface finishing (by shaving or by milling). The wear experiments were performed with two torque stages: 135 N.m (running-in) and 302 N.m (steady-state), and the test temperature was 90oC. The wear resistance was determined by using image analysis. In order to determine the specific film thickness, the Rq roughness and the minimum oil thickness were measured at each test stop. After the experiments were completed, it was possible to confirm that, for both manufacturing processes, the boundary lubrication regime was adopted at the tooth flank and the specific film thickness presents a different behavior when compared to addendum, pitch diameter and deddendum regions. The wear of the gears flank depended on the lubricant film thickness and it was higher with milled gears.
Key words: Contact fatigue; Gears; Pitting; Shaving, Specific film thickness.

INFLUENCIA DA DISTRIBUIÇÃO DE TENSÕES NO CONTATO E DA ESPESSURA ESPECÍFICA DE FILME NA RESISTÊNCIA AO DESGASTE DE ENGRENAGENS DE DENTES RETOS DURANTE ENSAIOS DE PITTING

Resumo
Um dos principais mecanismos de dano em engrenagem é a formação de *pitting* (crateração) e *spalling* (lascamento) no flanco dos dentes. Vários fatores apresentam influência significativa na formação destes danos, tais como: nível de tensão no contato; tipo de perfil de dente; velocidade relativa no contato, acabamento superficial e as condições de lubrificação. Este trabalho apresenta uma observação global de todos esses parâmetros, realizada para explicar os fenômenos relacionados aos mecanismos de desgaste. O equipamento de teste usa o princípio de recirculação de energia, e é comumente conhecido como equipamento tipo FZG. As engrenagens são fabricadas com a geometria do tipo C, com perfil modificado. As engrenagens foram feitas a partir do aço AISI 8620 e foram submetidfas a dois tipos de acabamento superficial (*shaving* ou fresagem). Os ensaios de desgaste foram realizados com duas níveis de carregamento: 135 Nm (*running-in*) e 302 Nm (*steady-state*), e à temperatura de ensaio foi de 90°C. A resistência ao desgaste foi determinada por análise de imagem. Para determinar a espessura específica de filme, a rugosidade Rq e a espessura mínima de óleo foram medidos a cada parada de teste. Após a realização dos experimentos, foi possível confirmar que, para ambos os processos de fabricação, o regime de lubrificação atuante em todo o flanco dos dentes foi o limite (*boundary lubrication*) e a espessura específica de filme apresenta um comportamento diferente nas regiões do adendo, diâmetro primitivo e dedendo. O desgaste das engrenagens flanco foi depende da espessura do filme lubrificante e foi maior para as engrenagens fresadas.
Palavras-chaves: Fadiga de contato; Engrenagens; *Pitting*; *Shaving*; Espessura específica de filme.

[1] *Technical contribution to the First International Brazilian Conference on Tribology – TriboBr-2010, November, 24th-26th, 2010, Rio de Janeiro, RJ, Brazil.*
[2] *Technical Suport Engineer, COSAN (Fuels and Lubricants)*
[3] *Graduated Student, Mechanical Engineering, Federal University of Technology - Paraná (UTFPR)*
[4] *Master of Mechanical Engineering, Cia Paranaense de Energia (COPEL)*
[5] *Doctor in Engineering, Federal University of Technology - Paraná (UTFPR)*

ISSN 2179-3956

1 INTRODUCTION

The gear teeth can fail for basically two modes: bending fatigue at the root of the teeth or by contact fatigue on the flank of the teeth. The contact fatigue is caused by tension developed in the contact between the flanks of the teeth, which after many cycles, causes of cracks. The conditions of contact are responsible for nucleation of these cracks in the surface or sub-surface regions of the flanks of the teeth. The cracks propagation may result in failure by pitting and/or spalling.(1)

The contact stresses on surfaces non-compliant, as the case of gears, can be determined by analytical equations based on the theory of elasticity developed by Hertz in 1881.(2) For this, usually the contact between two teeth is compared to the contact between two cylinders with radii equivalent to the radius of curvature at the contact point. It's very important to find which parameters of the tribological system affect the intensity of the hertzian stresses along the line of action. Among the main factors of influence can be mentioned: the geometric profile of the tooth flank (modulus, number of teeth, pressure angle), the gear materials, the lubricant, the load transmitted and kinematics of the movement.

The surface finishing has a strong influence on the life of the gears and the roughness behaves as a stress concentration factor for crack initiation, so this issue is relevant to the analysis of the wear of gear flanks. Several studies have been conducted to verify the effect of the roughness on the resistance to contact fatigue. According Zafosnik et al.(3) in rolling and sliding contact, the fatigue strength depends on many factors such as stress and strain elasto-plastic, material properties, physic-chemical properties of lubricant, surface roughness, stress residual and kinematics of contact. The surface cracks could be initiated near the surface deformation in the region of maximum shear stress caused by cyclic rolling-sliding contact, or alternatively near defects such as notches or scratches.

The load sharing function defines how the load distribution will occur along the gear contact. The use of this function is important to identify which tooth regions will be fully supporting the efforts transmitted. Figure 1 shows the two main load sharing forms.(4)

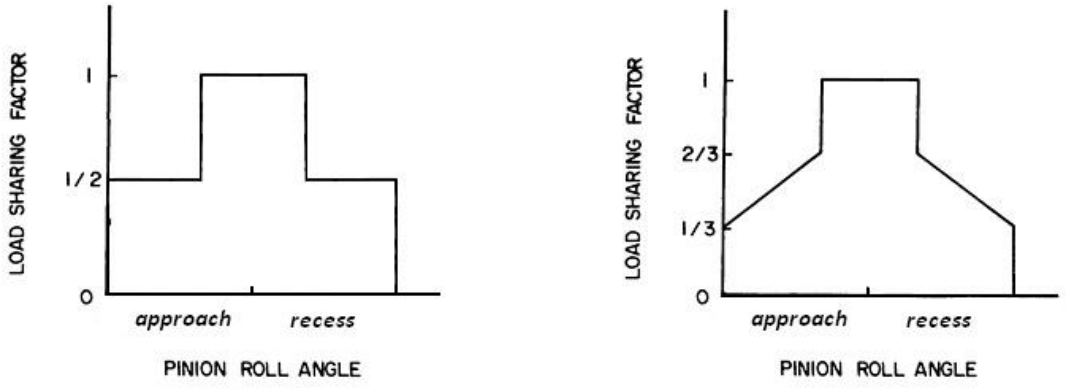

Figure 1 - Plot of load-sharing factor versus pinion roll angle. (a) Instantaneous mode, (b) influenced by the lubricant and deformation in the tooth.(4)

It is known that from the gear LPSTC (low point single tooth contact) to the HPSTC (high point single tooth contact), there is only a geared pair, that is, regardless of the load sharing function used, the normal force for this region will always be equal to the maximum normal force. Below the LPSTC and above the

ISSN 2179-3956

HPSTC there is more than one pair in contact. Therefore, the load sharing function becomes important to determine such forces. Figure 2 illustrates the LPSTC and HPSTC points for a gear tooth and the regions where the load sharing function - ***f(d)*** - will take place.

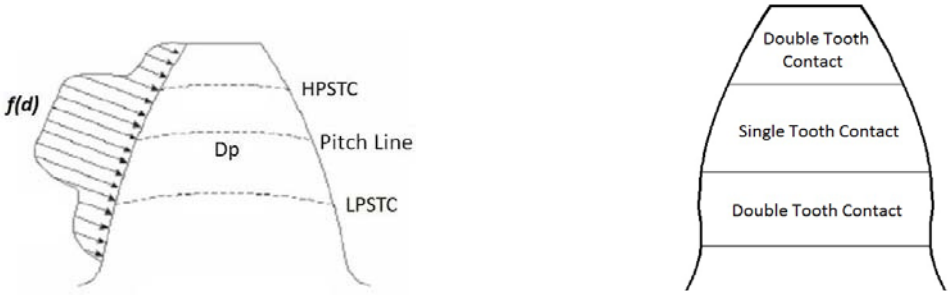

Figure 2 – Schematic pictures of LPSTC, HPSTC, pitch line and load sharing function - *f(d)*.[5]

Three steps are identified in the gear movement kinematics, as shown in Figure 3. At the beginning, the contact occurs through a combination of rolling and sliding (friction) between the teeth. In the pitch diameter region there is simple rolling, and it occurs again after sliding and rolling.

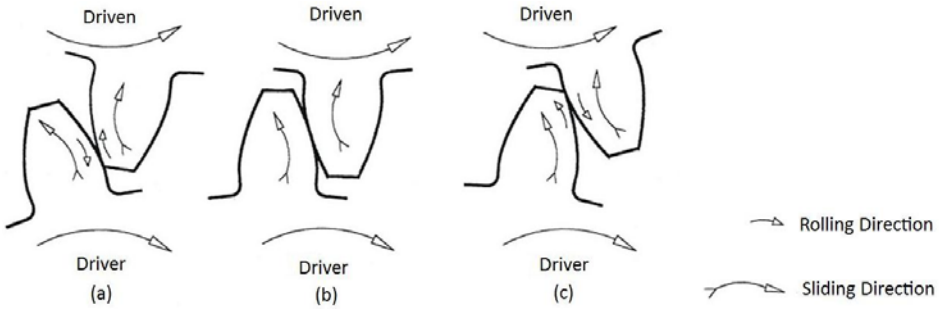

Figure 3. Meshing of spur gears showing the directions of rolling and sliding (friction). (a) Approach, (b) pitch diameter and (c) end of the meshing.[6]

The friction force causes changes in the stress field generated by contact between bodies, having great influence on contact fatigue failure. Among the friction models describing for gears in contact, we can call attention to: the equation of DIN 3990.[7] the equation described by ISO 6336,[8] the model proposed by Michaelis, the expression of Kelly and an equation for gear FZG proposed by Castro.[9] It is known from studies by Honh[10] that friction also suffers strong influence of the types of additives present in the lubricant. Another important factor presented by Honh and Michaelis [10] is related to the coating on the gears. Thus it can be stated that the proposed models may have some changes when working with or lubricants fortified with gears that have coatings.

Lubrication aims to introduce a film of low shear strength, which ends up weakening the resistance of these joints, reducing friction. In some cases, the lubricant may not completely prevent contact between the asperities, although it may reduce the severity of it. In other situations, the lubricant completely separates the surfaces and not formed asperities joints. Thus, a greater or lesser extent, the use of lubricants will always reduce the wear rate, and this will be a direct function of this type of lubrication. Norton[1] has said that there are basically three different regimes of lubrication: hydrodynamic lubrication (HD), the elastic-hydrodynamic (EHD) and

ISSN 2179-3956

boundary lubrication. In many cases a mixed condition of lubrication refers to the transition between EHD and boundary lubrication.

The contact between the surfaces of gear teeth is a "non-conformal", ie nominally involves a line or point contacts generating small concentrated area. Under these conditions the condition of lubrication is the predominant elasto-hydrodynamic - EHD. When there is breakage of the oil film, the lubrication regime becomes the boundary lubrication, where almost the entire load is supported by the asperities.(6)

The specific film thickness (λ) determines the lubrication conditions.(6) This parameter depends only on the minimum lubrication film thickness and surface roughness. For $\lambda > 3$, a full fluid lubricant film separates the two surfaces; the contact between asperities is negligible, and both the friction and the wear should be very low. However, many non-conformal contacts operate with $\lambda < 3$. For $1 < \lambda < 3$, the lubrication condition is partial or mixed EHD. Under these conditions, some contact between the asperities will occur, and the wear will be greater than in conditions where a full fluid lubricant film is present.(11)

The main objective of this work is monitoring changes in the contact conditions (hertzian pressures, film thickness, and friction) along the mesh while testing the contact fatigue of spur gears made from AISI 8620 hardened steel, originated from two different surface finishing kinds: shaving and milling.

2 EXPERIMENTAL PROCEDURE

2.1 Materials

The material used in the manufacture of spur gears is steel AISI 8620. The gears were machined and subjected to heat and thermo-chemical treatment in Wiser Pichler & Cia Ltda. The treatments are shown schematically in Figure 4.

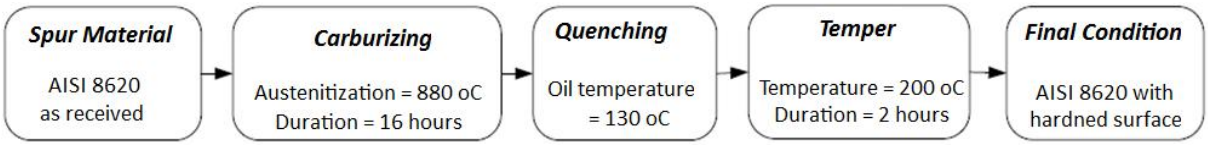

Figure 4 - Treatment sequence performed on AISI 8620 steel.

In Figure 5 are shown images (macro and micrography) of the teeth after a chemical etching with 5% Nital solution. In Figure 5 (a) you can see the hardened layer thickness is shown in Table 2. Figure 5 (b) shows the resulting microstructure in AISI 8620 steel after thermal treatments, consisting of martensite with some retained austenite. The final layer hardness is 40 HRc.

ISSN 2179-3956

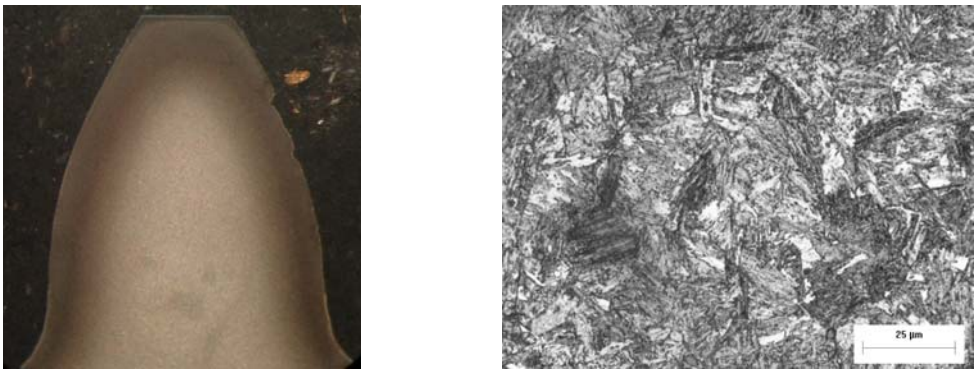

(a) (b)

Figure 5 - Macro and micrography of a pinion tooth. (a) Carburized layer, (b) Martensitic microstructure with some retained austenite.

Table 2 - Thickness of hardened layer (mm)

Milling		Shaving	
Pinion	Wheel	Pinion	Wheel
1,7 ± 0,2	1,5 ± 0,1	1,4 ± 0,1	1,5 ± 0,2

The lubricating oil used was ISO VG 100. The gears are dip lubricated with an oil volume of 1.5 l. After each step of the tests it was removed and replaced with new oil to the debris generated in the previous step did not influence the formation of pitting (by indentation). The main properties of the lubricant are shown in Table 3.

Table 3 - ISO VG 100 characteristics in two temperatures

	Unit.	**Running-in**	**Pitting Steps**
Temperature	(^{o}C)	60	90
Absolute viscosity - η	(cSt)	39,9	14,6
Pressure-viscosity coefficient - ζ	(in^2/lbf)	0,000136	0,000112
Specific Weigth – ρ	(kg/m^3)	855,7	840,0

2.2 Tests Methodology

In contact fatigue tests, FZG type C spur gears are used and their characteristics are shown in Table 4.

Table 4 - Characteristic of FZG type C gears and AISI 8620 properties

Parameter	**Unit.**	**Pinion**	**Wheel**
Number of teeth (Z)	-	16	24
Module (m)	mm	4,5	
Center Distance	mm	91,5	
Pressure angle (α)	^{o}	20	
Face width	mm	14	
Addendum modification	-	+0,182	+0,171
Addendum diameter	mm	82,45	118,35
Hardness	HRc	40 ± 1	
Young Modulus - E	GPa	205	
Poisson Coefficient - ν	-	14	

The gears used as samples were tested in the FZG-machine using a procedure similar to that proposed by the Institute FZG[12] for testing of pitting. In this method, besides the geometrical characteristics of the gears, are also indicates forms of

ISSN 2179-3956

loading for the stages of running-in and pitting test. The stages of loading used are presented in Table 5.

Table 5 - Stages of loading and speed used in fatigue tests of contact

FZG load	Stage of test	Wheel speed (rpm)	Torque (N.m)	Contact Pressure (MPa)
k6	*running-in*	1450	135,3	1153,8
k9	*pitting*		302,0	1723,8

Figure 6 shows the sequence of the methodology used in the experiments of contact fatigue in gears. At the end of testing, each gear (four pairs) was subjected to 7,48 x 10^6 cycles (pinion) and 4,99 x 10^6 cycles (wheel) of loading.

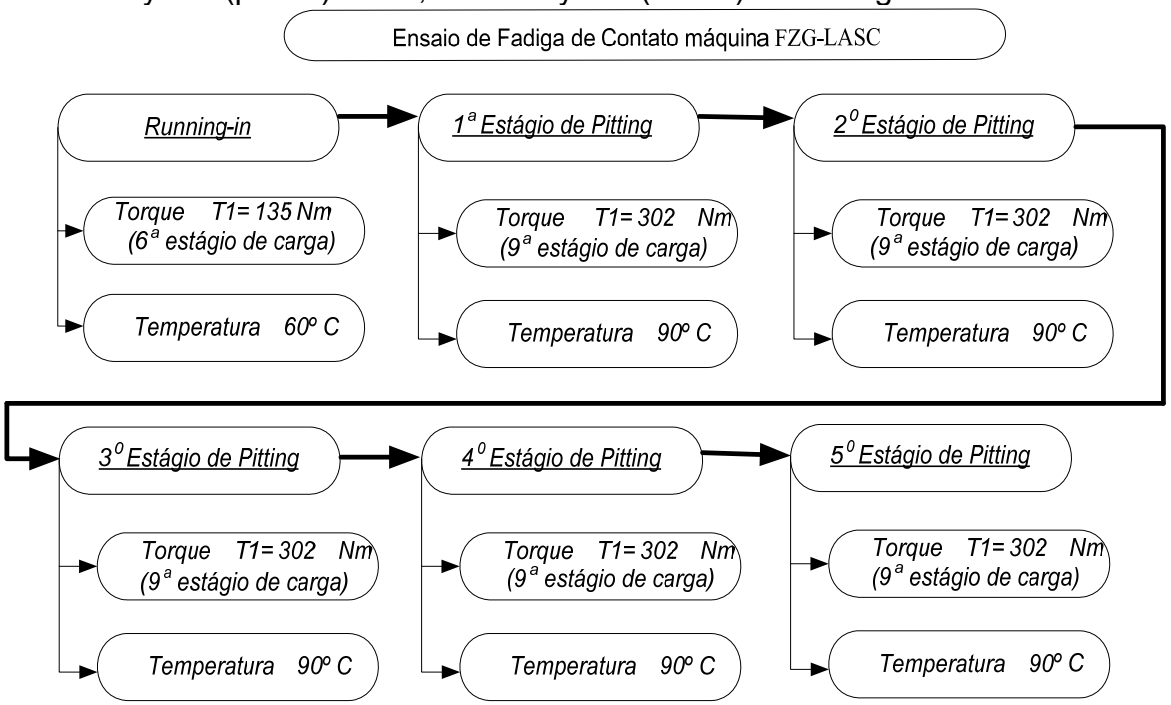

Figure 6 - Operating conditions used in fatigue contact tests.

2.3 Damaged by Pitting

Macroscopic images were made from the gear teeth flank, on condition before of running-in and after each step of the fatigue tests, so that one could observe the evolution of damage in the flanks with the cycles of loading.

(a) (b) (c)

Figure 7 - Evolution of damage to a tooth of a machined gear. (a) as received, (b) after 4th pitting step and (c) after 5th pitting step.

ISSN 2179-3956

To quantify the pitting damaged area, have been used images of flank of teeth. In this procedure was performed in all the damaged teeth of each gear. The total damage of all the teeth of a gear was divided by the total active area of all flank and this value, is called in this work, of average percentage of damage. Figure 7 shows an example of evolution of damage in a tooth.

2.4 Roughness

To determine the roughness of gear teeth, measurements were made on the flank of the teeth in the axial direction (parallel to the axis of gear). Were randomly selected five teeth of each pinion and wheel. With the roughness values measured in these teeth, after each fatigue test, were performed two different types of statistical analysis: average roughness around the flank (see Table 6) and roughness of the tooth by region (addendum, pitch diameter and deddendum).

Table 6 - Surface finish at the begin of the tests and after running-in period

	Roughness Parameters			
	Milling		*Shaving*	
	As receveid	After running-in	As receveid	After running-in
Ra (μm)	1,57 ± 0,13	0,88 ± 0,14	0,92 ± 0,08	0,51 ± 0,09
Rvk (μm)	2,5 ± 0,5	1.51 ± 0,14	1,4 ± 0,2	1,04 ± 0,17
Rsm (mm)	0,07 ± 0,01	0,12 ± 0,02	0,04 ± 0,01	0,07 ± 0,01

Table 6 shows that there was a marked reduction in roughness after running-in stage for the two types of surface finish (milling and shaving).

2.5 Specific Film Thickness

Norton[1] shows that the specific film thickness (λ) in contact gear teeth can be calculated as Equation 1. In this equation, $\boldsymbol{h_{min}}$ is the minimum thickness of the lubricant film and $\boldsymbol{R_{q1}}$, $\boldsymbol{R_{q2}}$ the values of root mean square (RMS) roughness of each surface contact (pinion-wheel).

$$\lambda = \frac{4}{3}.\frac{h_{\min}}{\sqrt{R_{q1}^2 + R_{q2}^2}} \tag{1}$$

To determine the minimum thickness (Equation 2) are considered the following parameters: transverse load (***P***), the width of the gear (***b***), the average speed (***U***), the absolute viscosity of lubricant at atmospheric pressure and operating temperature (η_o), the coefficient pressure-viscosity (ς),is the equivalent radius of curvature at the contact point of teeth ($\boldsymbol{R'_{eq}}$) and the effective young modulus (***E'***).

$$h_{\min} = 2{,}65.R'_{eq}.(\varsigma.E')^{0.54}.\left(\frac{\eta_o.U}{E'.R'_{eq}}\right)^{0.7}.\left(\frac{P}{b.E'.R'_{eq}}\right)^{-0.13} \tag{2}$$

2.6 Local Friction Coefficient

To calculate the friction coefficient at each point of the flank of gear teeth on the contact path, was used the Michaelis[13] equation, which is shown in Equation 3.

ISSN 2179-3956

$$\mu_{MIC} = 0.171\left(\frac{W_L}{R'_{eq}.V_R}\right)^{0.2}.\eta_o{}^{-0.05}\left(\frac{R_{aEq}}{d_1}\right)^{0.25}.X_L.X_C \quad (3)$$

In his proposal, Michaelis believes the following parameters: the specific load (***W_L***) in N/mm, the pinion diameter (***d_1***); the speed of rolling (***V_R***); the equivalent arithmetic average roughness of two surfaces in contact (***R_aEq***), the correction factor for the presence of additives in lubricant (***X_L***) and the correction factor for gears coated on the surface (***X_C***). In this work ***X_L***= 1 (lubricant without additives) and ***X_C***=1 (gears without coated).

At each point of the flank of gear teeth on the contact path, several parameters changes. Listed below are the formulations for each parameter that changes along the contact path.

- Equivalent arithmetic average roughness of two surfaces in contact:

$$R_{aEq} = \left(\frac{R_{a1} + R_{a2}}{2}\right) \quad (4)$$

- Equivalent radius of curvature at the contact point of teeth:

$$R'_{eq} = \left(\frac{1}{R_{1i}} + \frac{1}{R_{2i}}\right)^{-1} \quad (5)$$

- Speed of rolling:

$$V_R = \left(2 + \Gamma_y - \frac{\Gamma_y}{i}\right).V.sen\,\alpha \quad (6)$$

In the Equations 4, 5 and 6, the relevant parameters are: arithmetic average roughness of each tooth (***R_a1***, ***R_a2***); tangential speed (***V***); the gear ratio (***i***) and dimensionless parameter measure in contact mesh line (Γ_y). This parameter represents the distance from pitch point to point contact considered.

2.7 Stress Contact

To calculate the stress contact on the flank of teeth is use the analytical solution, proposed by Hertz,[1] to contact between two cylinders with radius equal the curvature radius of the teeth in each point in contact. The contact-patch half-width (*a*) is them found (Equation 7):

$$a = \sqrt{\frac{4}{\pi}.\frac{F_n}{b}.\frac{R'_{eq}}{E'}} \quad (7)$$

The zoom in contact zone will look as shown in Figure 8. The contact pressure (***p_máx***) is a maximum at the center and zero at the edges. The value of maximum pressure is obtained with Equation 8.

ISSN 2179-3956

$$p_{máx} = \frac{2 \,.\, P}{\pi . a . b} \tag{8}$$

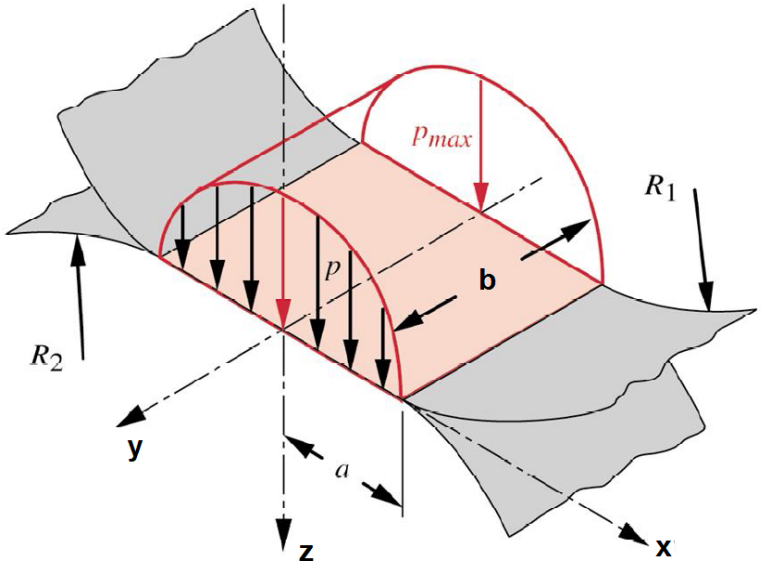

Figure 8 – Ellipsoidal-prism pressure distribuition and contact zones in cylindrical Hertzian contact.[1]

In all points of contact there is the possibility of sliding as well as rolling at the interface. The presence of tangential sliding forces (friction force) has a significant effect on the stress compared to pure rolling or static pressure.[1]

The contact geometry is as shown in Figure 8 with the ***x*** axis aligned to the direction of motion, the ***z*** axis radial to the teeth (thickness) and the y axis axial to the teeth (face width). The normal stresses (σ_n) due to the loading $\boldsymbol{p_{máx}}$ in the surface (when z = 0), are:

if $|x| \le a$ then $$\sigma_{xn} = -p_{máx} \cdot \sqrt{1 - \frac{x^2}{a^2}} \tag{9}$$

if $x < -a$ or $x > a$ then $$\sigma_{xn} = 0 \tag{10}$$

and $$\sigma_{xn} = \sigma_{zn} \quad , \quad \tau_{xz_n} = 0$$

The tangential stresses (σ_t) due the frictional force in the surface (when z = 0 and μ_{MIC} = friction coefficient), are:

if $x \ge a$ then $$\sigma_{xt} = -2\mu_{MIC} \cdot p_{máx} \left(\frac{x}{a} - \sqrt{\frac{x^2}{a^2} - 1} \right) \tag{11}$$

if $x \le -a$ then $$\sigma_{xt} = -2\mu_{MIC} \cdot p_{máx} \left(\frac{x}{a} + \sqrt{\frac{x^2}{a^2} - 1} \right) \tag{12}$$

ISSN 2179-3956

if $|x| \le a$ then $$\sigma_{xt} = -2\mu_{MIC} \cdot p_{máx} \cdot \frac{x}{a} \quad (13)$$

and

$$\sigma_{zt} = 0$$

if $|x| \le a$ then $$\tau_{xz_t} = -\mu_{MIC} \cdot p_{máx} \cdot \sqrt{1 - \frac{x^2}{a^2}} \quad (9)$$

if $x < -a$ or $x > a$ then $$\tau_{xz_t} = 0 \quad (10)$$

The total stress on each Cartesian plane is found by superposing the components due to the normal and tangential loads (Equation 14):

$$\sigma_x = \sigma_{xn} + \sigma_{xt} \qquad \sigma_z = \sigma_{zn} + \sigma_{zt} \qquad \tau_{xz} = \sigma_{xzn} + \sigma_{xzt} \quad (14)$$

For short gears in plane stress, σ_y is zero.

3 RESULTS

3.1 Running-in Period

The running-in period aims at equalizing the contact area and stabilizing such parameters as the friction coefficient. Figure 10 shows the friction coefficient along all points of contact during meshing, based on the pinion diameter. It can be observed that, during the running-in test, there is a drop in the friction coefficient for both milling and shave finishes. This fact is related to the reduction of surface roughness of the flank during the tests (see Table 6).

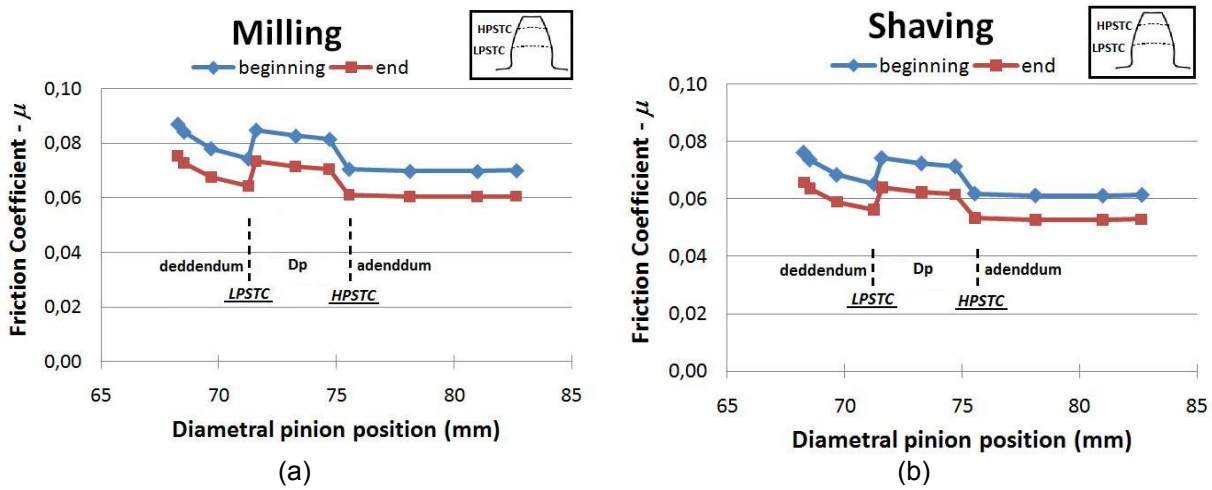

Figure 10. Variation in friction coefficient on the contact path. (a) Milling, (b) Shaving.

ISSN 2179-3956

Figure 11 shows the roughness profile measured in the region of pitch line of a gear with finishing by shaving, before and after the period of running-in. Both the reduction in height of the roughness (Ra) and the increased amount of peaks (Rsm) provides a growth in the real area of contact and a local reduction of stress state on the surface. Similar results were found by Cardoso et al.[14] in nitrided gears with lubricant and two ISO VG 100 biodegradable ester fluids with low toxicity additivation.

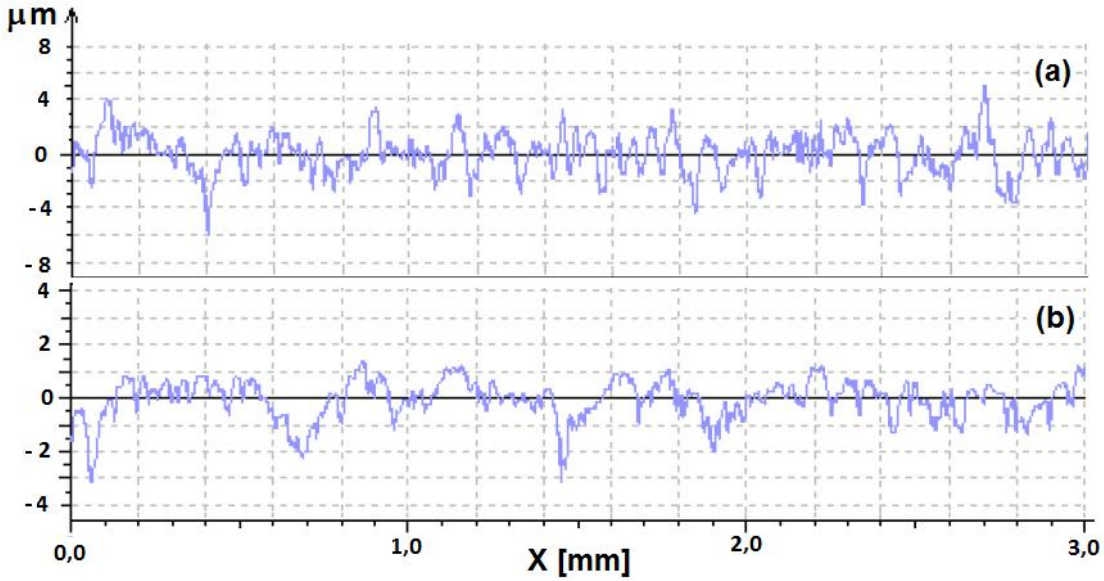

Figure 11. Pinion roughness profiles measured in the axial direction and near the pitch line of tooth with shave finishing. (a) As received, (b) After running-in tests.

Figure 10 shows that, along the contact path, the friction coefficient shows a decline in the region from the root to the top of the gear. But it is observed that friction values show a plateau in the region between the points LSPTC and HPSTC. This fact occurs due to the elevation of the normal load applied, which is defined by the load sharing function. This change in load can be seen clearly in Figure 12 (a). It also identifies a similar behavior of the distribution of contact stresses (σ_x) for the two test conditions. As presented by Krishnamurthy and Rao[15] is observed again the influence of torque and the presence of higher contact stresses in the region of deddendum.

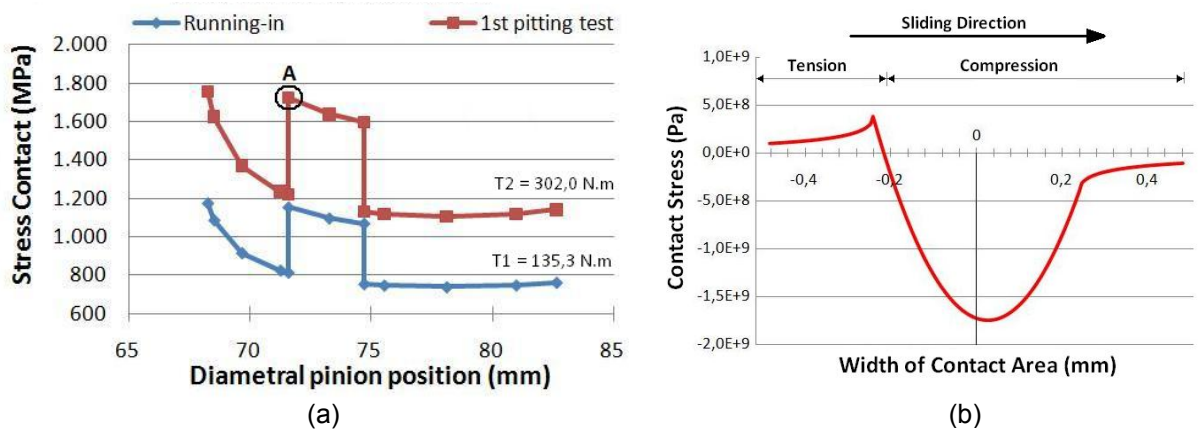

(a) (b)

Figura 12 - (a) Variation in contact stress on the contact path: running-in (T1) and pitting (T2), (b) Contact stress distribuition on aparent contact área (LSPTC of milling pinion in **A** point).

ISSN 2179-3956

Figure 12 (b) shows the distribution of stress (σ_x) in the apparent area of contact at **A** point (Figure 12 - a). It is observed that due to the efforts of friction, the maximum compressive stress is shifted in the direction of slip.

3.2 Thoth Flank Damaged Area

The quantification of the area of damage showed the influence of the roughness on the resistance to contact fatigue. As can be seen in Figure 13, milled gears were damaged from the second stage of pitting. From running-in until 3th pitting step, the shaving gears did not show any evidence of significant pitting. Thus, it can be said that by shaving the surface finish provides greater resistance to damage from the contact fatigue, especially by delaying the onset of damage.

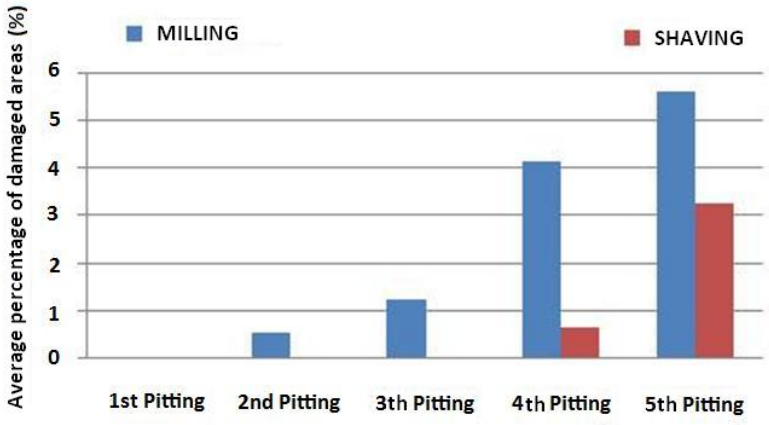

Figure 13 - Average percentage of damage in gears (pinion + wheel).

Despite changes in the parameters roughness and friction coefficient during the pitting tests, the values of maximum stress of contact does not show significant changes for both flank finishing: shaving and milling (Figure 14).

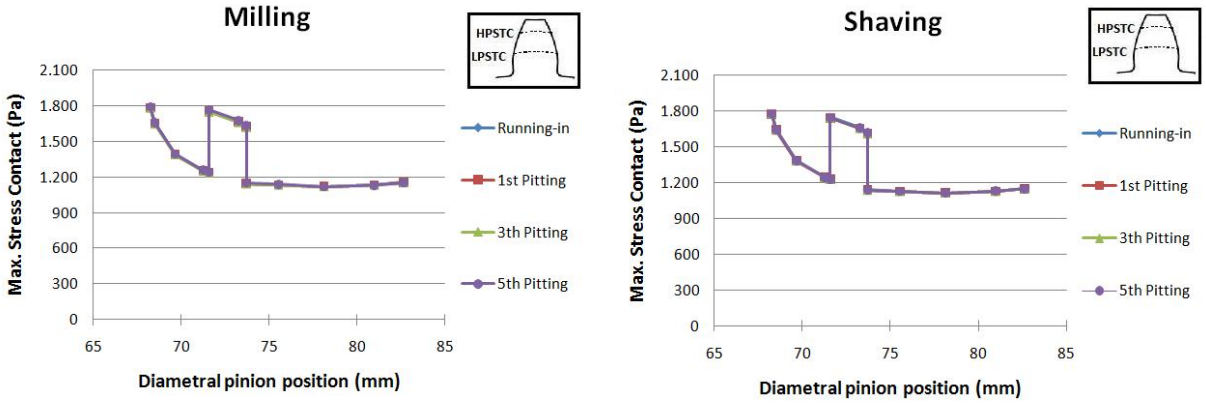

(a) (b)

Figure 14. Variation in contact stress on the contact path during pitting steps. (a) Milling, (b) Shaving.

The specific thickness of film (λ) of the gears in contact is a parameter able to explain the influence of types of surface finish on the wear of gears studied. It is observed in Figure 15 that the contact of milling gear, the specific film thickness is always less, thus making it the most severe load conditions. With the values of λ for all contact conditions can be stated that the lubrication regime is the EHD.

ISSN 2179-3956

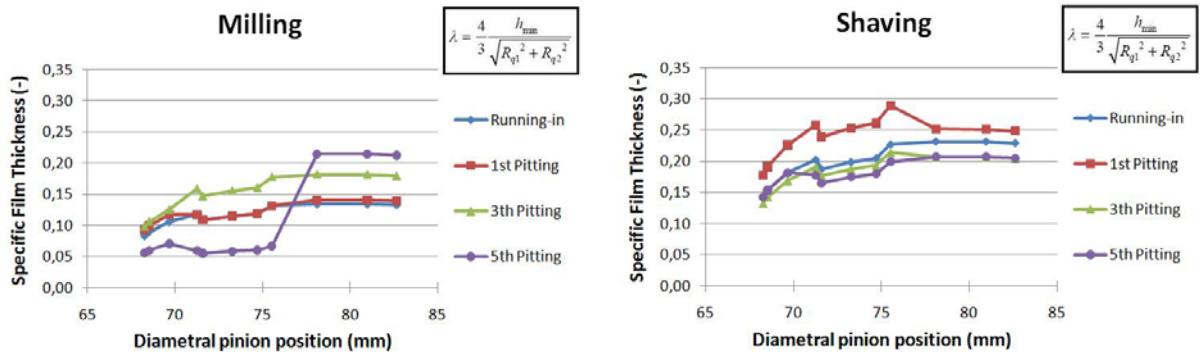

Figure 15. Variation in specific film thickness (λ) stress on the contact path during pitting steps. (a) Milling, (b) Shaving.

3.3 Discussion on Wear Mechanisms

Due to the kinematic characteristics of the contact of gear teeth's, lubricating conditions on the teeth are very different in addendum, pitch line and deddendum. When reviewing Figure 16 in relation to the regions of the flank is observed that the region of the pitch line and below, the specific thickness of film presents its lowest values. Added to this the fact that this parameter is directly linked to the state of the flank surface, can be stated as the conditions become more aggressive contact, the greater the occurrence of pitting, which reduces even over the film thickness and thus further intensifying the severity of the contact.

Figure 16 shows the evolution of Rvk roughness parameter, calculated from the measurements made in the axial direction of tooth flank during the pitting tests.

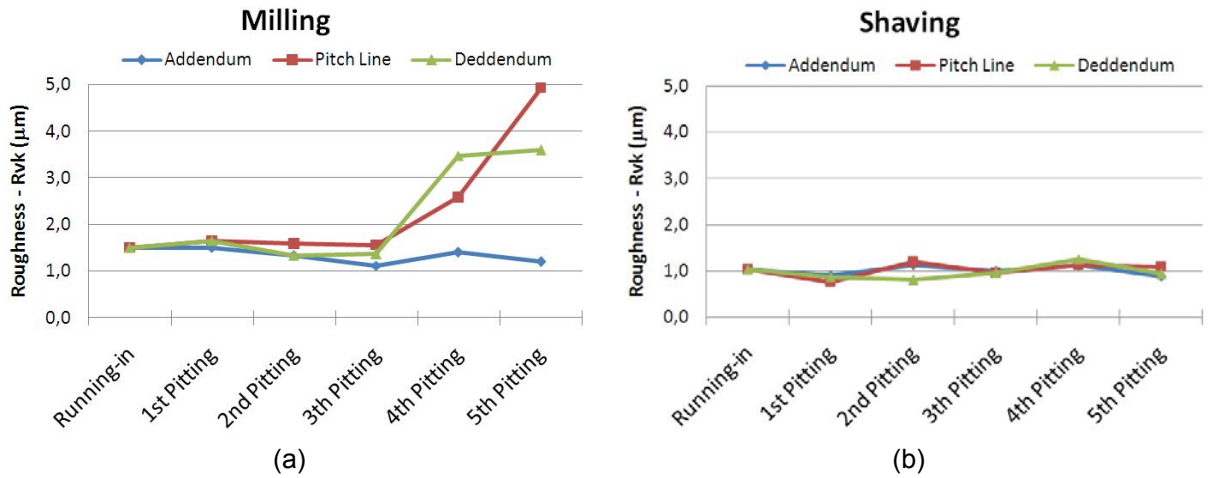

Figure 16 - Evolution of Rvk roughness parameter during the pitting tests. (a) Milling, (b) Shaving.

As found by Magalhães et al.[16], is observed in the milling gears that down the line of the pitch diameter is a significant increase in the Rvk parameters, indicating the presence of deep valleys, which are related to the presence of pitting on the flanks of the teeth. This enhancer effect of the aggressiveness of loading in the contact was not observed clearly in the shaving gears. However, it is possible to directly correlate the evolution of surface damage (Figure 13) both with parameter λ (Figure 14) and with Rvk (Figure 15).

Figure 17 (a) shows the sliding rate in the region of contact for the test gears type C. Comparing the regions of addendum and deddendum, you can identify that

ISSN 2179-3956

the sliding rate is higher in the region of the pinion deddendum. This fact also contributes to a severity of loading more intense.

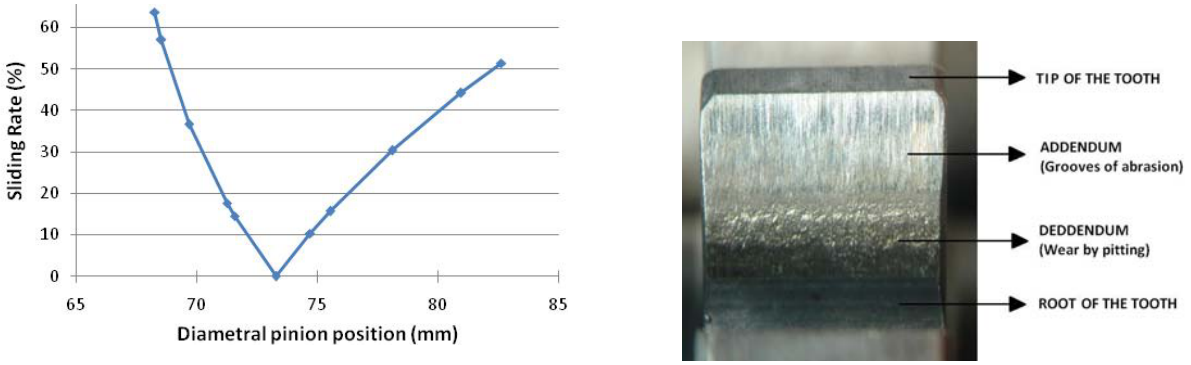

(a) (b)

Figure 17 – (a) Sliding rate in tooth contact. (b) Flank surface of milling pinion.

The surface of a tooth pinion milled after the 5th pitting step is shown in Figure 17 (b). The region of deddendum presented wear by pitting and spalling, typical mechanism at high stress and low film thickness. In the region of the addendum, the predominant wear mechanism is abrasive. However, this kind of damage was not addressed in this work.

4 CONCLUSIONS

The results obtained allow the following conclusions:

1. The surface finishing has a strong influence on the origin of contact fatigue damage (pitting and spalling). The gears with shaving showed better wear resistance than the nail, since they delay the initiation of sub-surface cracks
2. A more uniform load distribution on the teeth flank, achieved with lower Ra and higher Rsm values lead to increased wear resistance.
3. The results of specific film thickness (λ) show that the lubrication regime is severe for both gear finishes, shaving and milling, along the entire contact path.
4. The gears manufactured by shaving have higher λ values, i.e. the contact is less severe than that of milled gears, thus providing a better load support.
5. The combined use of techniques for monitoring by images and roughness measurement at each test step proved very effective in promoting understanding of the contact fatigue phenomena in gears.
6. The load-sharing function showed to have great influence in the regional deterioration of the teeth flank and may be accompanied by roughness measurements in the axial direction of the gears.
7. The identification of wear mechanisms by microscopic observation of the teeth flanks surface has confirmed the evidence of roughness, contact stresses, sliding rate, and specific film thickness parameters.

Acknowledgements

The authors would like to express their sincere gratitude to the support from National Scientific and Technological Development Council (CNPq Project 134251/2007-5), Surface Phenomena Lab. (LFS-EPUSP) and the companies: WEG Motores S.A., Wieser & Pichler Cia. Ltda, COSAN (Fuels and Lubricants) and Fundições Tupy Ltda.

ISSN 2179-3956

REFERENCES

1 NORTON, R. L., Projeto de Máquinas: uma abordagem integrada, 2ª Ed, Editora Bookman, p.414 – 425, 2004.
2 STACHOWIAK, G. W., BATCHELOR, A. W., Engineering Tribology, Elsevier Butterworth-Heinemann, p. 282 – 298, 2005.
3 ZAFOSNIK, B.; GLODEZ, S.; ULBIN, M.; FLASKER, J., A fracture mechanics model for the analysis of micro-pitting in regard to lubricated rolling–sliding contact problems, International Journal of Fatigue, vol. 29, p. 1950–1958, 2007.
4 ASM, ASM Handbook Volume 18: Friction, Lubrication and Wear Technology, ASM International, 1992.
5 IMREK, H., Performance improvement method for Nylon6 spur gears Tribology International 42, p. 503–510, 2009.
6 WALTON, D.; GOODWIN, A. J., The wear of unlubricated metallic spur gears Wear 222, p.103–113, 1998.
7 DIN 3990-4 Calculation of load capacity of cylindrical gears; calculation of scuffing load capacity, 1987
8 ISO 6336-1 Calculation of load capacity of spur and helical gears - Part 1: Basic principles, introduction and general influence factors, 1996.
9 CASTRO, M. J. D., Gripagem de engrenagens FZG lubrificadas com óleos base. Novos critérios de gripagem globais e locais. Doctoral Thesis, Faculdade de Engenharia, Universidade do Porto, 2004.
10 HOHN, B. R.; MICHAELIS, K., Influence of oil temperature on gear failures. Tribology International 37, p.103-109, 2004.
11 HUTCHINGS, I. M., Tribology: friction and wear of engineering materials, Ed. Butterworth – Heinemann. Oxford, p. 273, 1992.
12 FZG, Description of the pittingtest, Institute for Machine Elements – Gear Research Center, 1992.
13 CASTRO, M. J. D., SEABRA, J.H.O., Coefficient of friction in mixed film lubrication: Gears versus twin-discs. Proceedings of the Institution of Mechanical Engineers, Part J: Journal of Engineering Tribology Volume 221, Number 3, 2007.
14 CARDOSO, N. F. R.; MARTINS, R. C. A.; SEABRA J. H. O.; IGARTUA B, RODRIGUEZ J. C. C.; LUTHER R. D., Micropitting performance of nitride steel gears lubricated with mineral and ester oils.Tribology International 42, p.77– 87, 2009.
15 KRISHNAMURTHY, S.; RAO, A. R., Effect of sursulf treatment on the performance0.14% c steel gears. Wear, 120, p.289 – 303, 1987.
16 MAGALHÃES, L.; SEABRA, J.H.O.; MARTINS, R. C. A., Austempered ductile iron (ADI) gears: Power loss, pitting and micropitting, Wear, vol. 264, p. 839 – 849, 2007.